Envelope time reversal with a nonlinear time lens based on accelerating quasi-phase-matching

Oded Katz[*] and Alon Bahabad[†]
Department of Physical Electronics, School of Electrical Engineering, Fleischman Faculty of Engineering, Tel-Aviv University, Tel-Aviv 69978, Israel

(Received 11 August 2021; accepted 29 March 2022; published 14 April 2022)

We show theoretically and numerically that a time-reversed replica of the pump pulse envelope in a frequency converted signal can be achieved using a nonlinear time lens realized with an accelerating spatiotemporal quasi-phase-matching (QPM) modulation. The nonlinear process depends on a suitable combination of the input and output dispersion and acceleration rate of a quadratic spatiotemporal QPM modulation.

DOI: 10.1103/PhysRevA.105.043512

I. INTRODUCTION

A time-reversed pulse develops as though time runs backward; this has important applications such as disposing of distortions that happened at earlier times [1]. Time reversal allows for light detection, imaging, and focusing through complex media [2–5], having applications in a variety of disciplines, including plasmonics [6], medical ultrasound [2,3,7], superlensing [8], communication microwaves [9], ultrafast plasmonics [10], biological and terahertz imaging [11], spintronics [12], and quantum information and computing [13]. Nonlinear optical processes, such as nonlinear four-wave mixing [14–19] or time-modulated photonic structures [20–26], are the typical solution in optics for realizing time reversal.

One of the methods to realize time reversal relies on the use of the so-called time lens [27]. The basic idea behind the time lens is that the application of a quadratic phase modulation to a temporal waveform is analogous to the operation of a thin lens on a beam's transverse profile and is more generally based on the duality between beam diffraction in the spatial domain and pulse dispersion in the time domain. This is evident when considering simplified descriptions of electric fields corresponding to the transverse diffraction of a monochromatic beam and the dispersion of a pulsed plane wave with infinite transverse extent [28]. A time-lens element between two dispersive elements is thus equivalent to a spatial lens between two stretches of free space in the spatial domain, and thus a temporal imaging system can be constructed in an analogous way to a spatial imaging system [27–31]. Temporal imaging allows expanding or compressing the waveform of a temporal optical signal. When the magnification of the temporal imaging system is -1, time reversal of the envelope is achieved [32].

To realize the time lens, a quadratic phase modulation needs to be added to the waveform. This can be realized by optical frequency mixing with an appropriate chirped signal [32]. When considering such a process, it is important to make sure that it is phase matched [33,34] to enable efficient interaction, which is relevant to time reversal as well [35]. However, due to dispersion, phase matching is not always possible and an alternative method known as quasi-phase-matching (QPM) can be used. With QPM a parameter relevant to the process is modulated macroscopically to allow replacing the phase-matching condition, which is usually a requirement, with a less restrictive condition [36]. Thus with spatial modulation, momentum conservation can be replaced with quasimomentum (crystal momentum) conservation, while temporal modulation through the application of a spatial modulation can replace energy conservation with quasienergy conservation. More generally, a spatiotemporal modulation can be applied to handle phase mismatch which is split between both spatial (momentum) and temporal (energy) components [37]. Such a QPM scheme was realized experimentally using a train of counterpropagating pulses serving as the QPM modulation [38]. With all-optical perturbations of a nonlinear optical mixing process, more complicated spatiotemporal modulations should be feasible. Such modulations can be realized by superposing optical pulses with chirp and/or different spatiotemporal couplings [39], allowing for accelerating QPM geometries with which different phase-matching conditions can be imposed at different times during the nonlinear interaction. Further realizations of accelerating QPM geometries have been proposed in [40] as a tool to manipulate the extreme nonlinear process of high-harmonic generation (HHG). The description of such processes can very well be incorporated as a perturbation in the nonlinear polarization via a geometrical term. With HHG this is trivial as intensity variations in the pump are translated to phase variations in the emission of the high harmonics. Such a mechanism that translates intensity variation to phase variation should also exist with second-harmonic generation (SHG). One option would be to employ rapid-phase disturbance of the nonlinear polarization term. Such a mechanism was first suggested for HHG [41] and later also for SHG [42]. Another option would be to use thermal effects; however, in that case only very slow temporal modulations could be supported.

[*]Also at Department of Physical Electronics, School of Electrical Engineering, Fleischman Faculty of Engineering, Tel-Aviv University, Tel-Aviv 69978, Israel.
[†]alonb@eng.tau.ac.il

Another work showed that such a modulation in the presence of group-velocity mismatch (GVM) between a fundamental harmonic (FH) and its second harmonic (SH) can imprint the square of the time-reversed waveform of the FH on the SH [43], realizing a nonlinear form of time reversal (nonlinear in the sense that the mapping is made from the *square* of the FH waveform). More importantly, accelerating QPM was shown to enable time-to-frequency mapping between a pump pulse and the generated harmonic radiation [44]. The last case is especially relevant to the present work as such a mapping is an integral part of a temporal imaging system based on the time lens [45] (similarly to the spatial frequency-to-coordinate mapping realized with a spatial lens). The mapping that was explored was between the square of the temporal waveform (not the temporal waveform itself) of a FH and the spectrum of its SH. In this work we show that, together with appropriate dispersive elements, the nonlinear time-to-frequency mapping with an accelerating QPM can be used as a nonlinear time lens in a temporal imaging system to realize imprinting of the square of the reversed temporal waveform of the FH on the SH, while GVM is not required in this case (as it was in Ref. [43]).

II. THEORY

In a nonmagnetic medium, the one-dimensional wave equation for the SH field $\tilde{E}_{2\omega_0}(z,\omega)$ in the frequency domain under the nondepletion approximation

$$\frac{\partial^2 \tilde{E}_{2\omega_0}(z,\omega)}{\partial z^2} + \beta^2(\omega)\tilde{E}_{2\omega_0}(z,\omega) = -\mu_0\omega^2\tilde{P}_{NL}(z,\omega), \quad (1)$$

where $\beta(\omega) = \frac{n(\omega)\omega}{c}$ is the wave number, $n(\omega)$ is the index of refraction, and $c = \frac{1}{\sqrt{\mu_0\varepsilon_0}}$ is the speed of light, with μ_0 and ε_0 the vacuum permeability and permittivity, respectively. The $\tilde{P}_{NL}(z,\omega)$ is the Fourier transform of the material second-order nonlinear polarization

$$P_{NL}(z,t) = \varepsilon_0\chi^{(2)}g(z,t)E_{\omega_0}(z,t)^2, \quad (2)$$

where $\chi^{(2)}$ is the second-order electric susceptibility, $E_{\omega_0}(z,t)$ is the FH electric field, and $g(z,t) = e^{i\Phi(z,t)}$ represents the QPM spatiotemporal modulation.

In order to facilitate a time-lens operation, the phase-modulation pattern $\Phi(z,t)$ needs to be quadratic along a coordinate τ in the frame moving at the FH pulse group velocity $\tau = t - \frac{z}{v_{g1}}$. This realizes a linear mapping for the instantaneous frequency $\Delta\omega(\tau) = -\frac{\partial\Phi(z,t)}{\partial\tau}$ from the time domain (for the square of the FH pulse shape) to the frequency domain (for the SH spectrum) in the form of $\Delta\omega(\tau) = a + b\tau$, with a (s^{-1}) and b (s^{-2}) the modulation parameters determining the displacement in the central frequency of the SH spectrum and the chirp rate of the modulation, respectively [44].

The instantaneous frequency $\Delta\omega(\tau)$ serves as the energy mismatch in the interaction, while $\Delta k(z) = \frac{\partial\Phi(z,t)}{\partial z}$ serves as the momentum mismatch. The phase-mismatch terms must obey the dispersion condition of the system [37]

$$\Delta k(\tau) = \Delta\omega(\tau)\frac{n(\omega_{SH})}{c} + \frac{2\omega_0}{c}\{n(\omega_0) - n(\omega_{SH})\}, \quad (3)$$

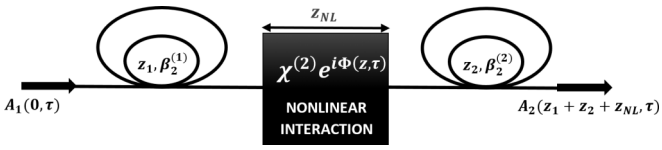

FIG. 1. Time-reversal configuration. An input pulse envelope of a FH first experiences a dispersive element of length z_1 and GVD $\beta_2^{(1)}$. It then propagates in a nonlinear medium in which a spatiotemporal modulation realizes a time lens between the square of the FH and the SH. Finally, the SH envelope undergoes dispersion over a length of z_2 with GVD $\beta_2^{(2)}$.

with $\omega_{SH} = 2\omega_0 - \Delta\omega(\tau)$. All these lead to a simple expression for the QPM modulation [44]

$$g(z,\tau) = e^{i\Phi(z,\tau)} = e^{i(\Delta k_0 z - a\tau - b\tau^2/2)}, \quad (4)$$

where $\Delta k_0 = \frac{2\omega_0}{c}[n(\omega_0) - n(\omega_{SH})]$ is the momentum mismatch when energy is conserved [33]. We note again that the temporal quadratic phase term $b\tau^2/2$ facilitates the nonlinear time lens. To set the central frequency of the SH field at $2\omega_0$, we choose $a = -bt_0$, with t_0 the middle of the FH pulse at the beginning of the nonlinear interaction.

We now consider the system depicted in Fig. 1 in which an input FH with envelope $A_1(z=0, t - \frac{z}{v_{g1}})$ propagating with group velocity v_{g1} meets a succession of elements: a dispersive element (which can be a fiber), a nonlinear medium in which the QPM modulation is applied, and another dispersive element. The two dispersive elements are characterized with propagation coefficients $\beta^{(1)}$ and $\beta^{(2)}$ and their corresponding group-velocity dispersion coefficients $\beta_2^{(1)} = \frac{d^2\beta^{(1)}}{d\omega^2}$ and $\beta_2^{(2)} = \frac{d^2\beta^{(2)}}{d\omega^2}$.

At the end of the first dispersion element, which is the start of the nonlinear element, at coordinate $z = z_1$, the field envelope in the Fourier domain is given by

$$\tilde{A}_1(z_1,\tilde{\omega}) = \tilde{A}_1(z=0,\tilde{\omega})G_1(z_1,\tilde{\omega}), \quad (5)$$

where $\tilde{\omega} = \omega - \omega_0$, with ω_0 the central frequency of the pulse; $\tilde{A}_1(z,\tilde{\omega}) = \mathcal{F}\{A_1(z,t)\}$ is the Fourier transform with respect to time t; and $G_1(z_1,\tilde{\omega})$ denotes the action in Fourier space of the first dispersive element and is given by

$$G_1(z_1,\tilde{\omega}) = e^{-i\alpha\tilde{\omega}^2}, \quad \alpha = \frac{z_1}{2}\beta_2^{(1)}, \quad (6)$$

where $\beta_2^{(1)}$ is the group-velocity dispersion (GVD) for the FH. Similarly, the second dispersive element acts on the SH

$$\tilde{A}_2(z_1+z_2+z_{NL},\tilde{\tilde{\omega}}) = \tilde{A}_2(z_1+z_{NL},\tilde{\tilde{\omega}})G_2(z_2,\tilde{\tilde{\omega}}), \quad (7)$$

$$G_2(z_2,\tilde{\tilde{\omega}}) = e^{-i\beta\tilde{\tilde{\omega}}^2}, \quad \beta = \frac{z_2}{2}\beta_2^{(2)}, \quad (8)$$

where $\beta_2^{(2)}$ is the GVD for the SH, with $\tilde{\tilde{\omega}} = \omega - 2\omega_0$. The field envelope in the time domain at $z = z_1$ is

$$A_1\left(z_1, t - \frac{z}{v_{g1}}\right) = \mathcal{F}^{-1}\{\tilde{A}_1(z=0,\tilde{\omega})G_1(z_1,\tilde{\omega})\}, \quad (9)$$

where $\mathcal{F}^{-1}$ stands for the inverse Fourier transform. The full electric field at $z = z_1$ is

$$E_{1,\omega_0}(z_1,t) = A_1\left(z_1, t - \frac{z_1}{v_{g1}}\right)e^{i(\omega_0 t - k_0 z_1)}, \tag{10}$$

where $k_0 = \frac{n(\omega_0)\omega_0}{c}$ is the FH wave vector and $n(\omega_0)$ is the index of refraction of the FH in the nonlinear medium. Under the nondepletion approximation, we can assume that this form of the FH would be kept for $z_1 < z < z_1 + z_{NL}$.

We now follow a procedure very similar to that reported in Ref. [44], in which the temporal envelope is represented with a Fourier series multiplied by a Gaussian window (whose function is to isolate one instance of the infinite train of pulses defined by the Fourier series):

$$A_1(z_1,t) = e^{-t^2/T^2}\sum_{n=-\infty}^{\infty} F_n e^{i\tilde{\omega}_n t}. \tag{11}$$

Here $\tilde{\omega}_n = \frac{2\pi n}{\tilde{T}}$ with an arbitrarily large time period $\tilde{T}$ and the F_n are the Fourier series coefficients for the periodic expansion of the envelope:

$$F_n = \frac{1}{\tilde{T}}\int_{-\tilde{T}/2}^{+\tilde{T}/2} A_1(z_1,t)e^{-i\tilde{\omega}_n t}dt. \tag{12}$$

For a valid representation we must require that $\tilde{T} \gg T \gg \tau_{1,0}$, with $\tau_{1,0}$ the temporal width of the envelope $A_1(z_1,t)$ at z_1. Assuming that $A_1(z_1,t)$ is nonzero only within $[-\tilde{T}/2, +\tilde{T}/2]$, we can write the Fourier transform of $A_1(z_1,t)$ as

$$\tilde{A}_1(z_1,\tilde{\omega}) = \int_{-\tilde{T}/2}^{+\tilde{T}/2} A_1(z_1,t)e^{-i\tilde{\omega}t}dt, \tag{13}$$

which immediately gives

$$F_n = \frac{1}{\tilde{T}}\tilde{A}_1(z_1,\omega_n). \tag{14}$$

As the parameter T can be set to be arbitrarily large, the shifting Gaussian function need not be moved together with the Fourier components when we describe the propagation of the envelope:

$$A_1(z_1, t - \frac{z}{v_{g1}}) \cong e^{-t^2/T^2}\sum_{n=-\infty}^{\infty} F_n e^{i\tilde{\omega}_n(t - z/v_{g1})}. \tag{15}$$

We will evaluate the spectrum of the SH electric field inside the nonlinear medium $z_1 < z < z_1 + z_{NL}$, where z_{NL} is the interaction length within this medium. Substituting the modulation phase function given by Eq. (4) and the fundamental electric field given by Eqs. (10) and (15) into the nonlinear polarization expression (2) and employing a Fourier transform in the time domain yields

$$\begin{aligned}\tilde{P}_{NL}(z,\omega) = &\sum_{n=-\infty}^{\infty}\sum_{m=-\infty}^{\infty}\frac{\sqrt{2\pi}\epsilon_0\chi^{(2)}}{\sqrt{\frac{4}{T^2}+ib}}F_nF_m\\ &\times\exp\left[-i\left(-\Delta k_0 + 2k_0 + \frac{-a+\tilde{\omega}_m+\tilde{\omega}_n}{v_{g1}}\right)z\right]\\ &\times\exp\left(-i\frac{1}{2}b\frac{z^2}{v_{g1}^2}\right)\exp\left(-\frac{(\Omega - b\frac{z}{v_{g1}})^2}{\frac{8}{T^2}+2ib}\right),\end{aligned} \tag{16}$$

where we defined $\Omega = \omega - 2\omega_0 + a - \tilde{\omega}_m - \tilde{\omega}_n$. Selecting T large enough such that $\frac{8}{T^2} \ll 2b$, we get

$$\begin{aligned}\tilde{P}_{NL}(z,\omega) = &\frac{\sqrt{2\pi}\epsilon_0\chi^{(2)}}{\sqrt{ib}}e^{-iK(\omega)z}\\ &\times\exp\left(i\frac{(\omega-2\omega_0+a)^2}{2b}\right)\\ &\times\left[a_1\left(z_1, -\frac{\omega-2\omega_0+a}{b}\right)\right]^2,\end{aligned} \tag{17}$$

where $K(\omega) = -\Delta k_0 + 2k_0 + \frac{\omega - 2\omega_0}{v_{g1}}$ and we define

$$\begin{aligned}&\left[a_1\left(z_1, -\frac{\omega-2\omega_0+a}{b}\right)\right]^2\\ &= \sum_{n=-\infty}^{\infty}\sum_{m=-\infty}^{\infty}F_nF_m\\ &\quad\times\exp\left(-i\frac{(\omega-2\omega_0+a)}{b}(\tilde{\omega}_n+\tilde{\omega}_m)\right)\\ &\quad\times\exp\left(i\frac{(\tilde{\omega}_n+\tilde{\omega}_m)^2}{2b}\right).\end{aligned} \tag{18}$$

We note that under the condition

$$F_t \equiv \tau_{1,0}^2 b \gg 1, \tag{19}$$

which is equivalent to the SH bandwidth being much wider than the FH bandwidth [44], we can approximate $[a_1(z_1, -\frac{\omega-2\omega_0+a}{b})]^2 \approx [A_1(z_1, -\frac{\omega-2\omega_0+a}{b})]^2$ by neglecting the terms $\exp[i\frac{(\tilde{\omega}_n+\tilde{\omega}_m)^2}{2b}]$ [44]. This condition is required to establish an accurate time-to-frequency mapping by the nonlinear section of the interaction. We would use this condition later on; however, we already note that it can be viewed as a near-field condition for a temporal Fresnel number [46]. To see this, we recall that the spatial Fresnel number is defined as $F = \frac{a_x^2}{L\lambda}$ for an optical wave at wavelength λ passing through an aperture with radius a_x and measured a distance L away. The space-time analogy is made by comparing a_x to $\tau_{1,0}$ and $L\lambda$ to $1/b$.

Now, using Eq. (18) in Eq. (1) with the boundary conditions $\tilde{E}_{2\omega_0}(z = z_1, \omega) = \frac{\partial\tilde{E}_{2\omega_0}(z=z_1,\omega)}{\partial z} = 0$, we get the SH electric field in the range $z_1 < z < z_1 + z_{NL}$,

$$\begin{aligned}\tilde{E}_{2\omega_0}(z,\omega) = &\sqrt{2\pi}R(z,\omega)\exp\left(i\frac{(\omega-2\omega_0+a)^2}{2b}\right)\\ &\times\left[a_1\left(z_1, -\frac{\omega-2\omega_0+a}{b}\right)\right]^2,\end{aligned} \tag{20}$$

where

$$\begin{aligned}R(z,\omega) = &-\frac{\mu_0\epsilon_0\chi^{(2)}}{\sqrt{ib}}\frac{\omega^2}{K(\omega)^2-\beta(\omega)^2}\\ &\times\left(-e^{-iK(\omega)(z-z_1)} + \cos[\beta(\omega)(z-z_1)]\right.\\ &\left.-i\frac{K(\omega)}{\beta(\omega)}\sin[\beta(\omega)(z-z_1)]\right).\end{aligned} \tag{21}$$

The term $R(z,\omega)$ leads to distortions of the time-to-frequency mapping caused by the FH's dispersion during the nonlinear interaction. For z values much smaller than the dispersion length $l_D = \frac{\Delta\tau_{1,0}^2}{\beta''}$, where β'' is the maximum group-velocity dispersion between the FH and SH in the nonlinear medium, the magnitude of $R(z,\omega)$ would be fairly constant in ω [44] and the time-to-frequency mapping would be fairly good (as long as $\tau_{1,0}^2 b \gg 1$ is also satisfied). In this case we would set $R(z,\omega) \approx R(z,2\omega_0) = R(z)$.

With these conditions, our nonlinear time lens can be considered as a thin lens. It is interesting to compare the dispersion length in our temporal domain to the diffraction of Gaussian beam in the spatial domain in which the characteristic length is the Rayleigh range $l_R = \frac{1}{2}kW_0^2$, where W_0 is the beam waist, analogous to the pulse duration, and the wave vector $k = 2\pi/\lambda$ is analogous to $1/\beta''$. A spatial lens can be considered optically thin if the lens thickness is small compared to the Rayleigh length.

For the following it is convenient to use the relation between the envelope and the field in the spectral domain:

$$\tilde{E}_{2\omega_0}(z,\omega) = \tilde{A}_2(z,\omega-2\omega_0)e^{-i2k_0(z-z_1)}. \tag{22}$$

By replacing $\omega - 2\omega_0 + a \to \nu$ in Eqs. (20) and (22) we get the spectrum complex envelope of the SH field

$$\tilde{A}_2(z,\nu-a) = r(z)\sqrt{2\pi}e^{i\nu^2/2b}a_1^2\left(z_1,-\frac{\nu}{b}\right), \tag{23}$$

where $r(z) = R(z)e^{i2k_0(z-z_1)}$. By substituting Eqs. (14) and (18) into Eq. (23) along with setting $\Delta\omega_n = \Delta\omega_m = \frac{2\pi}{T}$ we get

$$\tilde{A}_2(z,\nu-a) = r(z)e^{i\nu^2/2b}\frac{1}{(2\pi)^{1.5}}\sum_{n=-\infty}^{\infty}\sum_{m=-\infty}^{\infty} \times \tilde{A}_1(z_1,\omega_n)\tilde{A}_1(z_1,\omega_m)\exp\left(-i\frac{\nu}{b}(\tilde{\omega}_n+\tilde{\omega}_m)\right) \times \exp\left(i\frac{(\tilde{\omega}_n+\tilde{\omega}_m)^2}{2b}\right)\Delta\omega_n\Delta\omega_m. \tag{24}$$

We switch to the infinitesimal limit, with $\tilde{T}\to\infty$, $(\omega_n,\omega_m)\to(\omega',\omega'')$, and $(\Delta\omega_n,\Delta\omega_m)\to(d\omega',d\omega'')$ to yield

$$\tilde{A}_2(z,\nu-a) = r(z)e^{i\nu^2/2b}\frac{1}{(2\pi)^{1.5}}\int_{\omega'=-\infty}^{\infty}\int_{\omega''=-\infty}^{\infty}\tilde{A}_1(z_1,\omega') \times \tilde{A}_1(z_1,\omega'')\exp\left(-i\frac{\nu}{b}(\tilde{\omega}'+\tilde{\omega}'')\right) \times \exp\left(i\frac{(\omega'+\omega'')^2}{2b}\right)d\omega' d\omega''. \tag{25}$$

Finally, the spectrum complex envelope at the end of the output dispersion component is

$$\tilde{A}_2(z_1+z_2+z_{NL},\nu-a) = \tilde{A}_2(z_1+z_{NL},\nu-a)G_2(z_2,\nu-a), \tag{26}$$

where G_2 was defined in Eq. (8). Following further development in the time domain (see the Appendix for detailed computation) the SH field envelope is therefore

$$\begin{aligned} A_2(z_1+z_2+z_{NL},\tau) = {} & \frac{r(z_1+z_{NL})}{(2\pi)^{2.5}}e^{-i\beta a^2}e^{i(2\omega_0-a)(\tau_a-2\beta a)}\sqrt{\frac{\pi}{i(\beta-\frac{1}{2b})}}\exp\left(i\frac{\tau_a^2}{4(\beta-\frac{1}{2b})}\right) \\ & \times\int_{\omega'=-\infty}^{\infty}\tilde{A}_1(0,\omega')\exp\left[i\omega'^2\left(-\alpha+\frac{1}{2b}+\frac{\frac{1}{b^2}}{4(\beta-\frac{1}{2b})}\right)\right]\exp\left[i\omega'\left(\frac{-\frac{1}{b}}{2(\beta-\frac{1}{2b})}\right)\tau_a\right]d\omega' \\ & \times\int_{\omega''=-\infty}^{\infty}\tilde{A}_1(0,\omega'')\exp\left[i\omega''^2\left(-\alpha+\frac{1}{2b}+\frac{\frac{1}{b^2}}{4(\beta-\frac{1}{2b})}\right)\right]\exp\left[i\omega''\left(\frac{-\frac{1}{b}}{2(\beta-\frac{1}{2b})}\right)\tau_a\right] \\ & \times\left\{\exp\left[i\omega'\omega''\left(\frac{\frac{1}{b^2}}{2(\beta-\frac{1}{2b})}+\frac{1}{b}\right)\right]\right\}d\omega''. \end{aligned} \tag{27}$$

We now look for the conditions under which the output waveform could be called the time reversal of the input FH waveform (squared). This would be satisfied if the SH waveform had the same envelope profile (squared), with a reversed timescale (that is, $t\to -t$). The first condition we identify is eliminating the quadratic phase in the integrands of Eq. (27): $-\alpha+\frac{1}{2b}+\frac{\frac{1}{b^2}}{4(\beta-\frac{1}{2b})}=0$. This yields

$$\frac{1}{\alpha}+\frac{1}{\beta}=2b. \tag{28}$$

So Eq. (27) becomes

$$\begin{aligned} A_2(z_1+z_2+z_{NL},\tau) = {} & \frac{r(z_1+z_{NL})}{(2\pi)^{2.5}}e^{-i\beta a^2}\times e^{i(2\omega_0-a)(\tau_a-2\beta a)}\sqrt{\frac{\pi}{i(\beta-\frac{1}{2b})}}\exp\left(i\frac{\tau_a^2}{4(\beta-\frac{1}{2b})}\right) \\ & \times\int_{\omega'=-\infty}^{\infty}\tilde{A}_1(0,\omega')\exp\left[i\omega'\left(\frac{-\frac{1}{b}}{2(\beta-\frac{1}{2b})}\right)\tau_a\right]d\omega' \\ & \times\int_{\omega''=-\infty}^{\infty}\tilde{A}_1(0,\omega')\exp\left[i\omega''\left(\frac{-\frac{1}{b}}{2(\beta-\frac{1}{2b})}\right)\tau_a\right]\left\{\exp\left[i\omega'\omega''\left(\frac{\frac{1}{b^2}}{2(\beta-\frac{1}{2b})}+\frac{1}{b}\right)\right]\right\}\omega''. \end{aligned} \tag{29}$$

Note the striking similarity of Eq. (28) to the lens equation $1/u, +1/v = 1/f$ [where u (v) is the lens distance to the object (image) and f is the focal length], which describes the condition for imaging with a spatial lens. This analogy is well known for the time lens [27] and it is extended to the nonlinear time lens we present here as well. Note that in the case of diffraction during propagation before the spatial lens, the instantaneous spatial frequencies of a paraxial beam acquire a negative frequency chirp in the sense that the high spatial frequencies travel laterally faster than the low spatial frequencies. On the other hand, before the temporal lens and for normal dispersion ($\alpha, \beta > 0$), a pulse acquires a positive frequency chirp since the low frequencies travel faster than the high frequencies. Thus, in the sense that a lens needs to cancel out the natural chirping of the system that precedes it, our nonlinear time lens must have a sign of phase curvature different from that of a spatial lens in order to satisfy the temporal imaging condition. This is expressed in the minus sign in front of the quadratic term $b\tau^2$ in the QPM modulation geometry [Eq. (4)].

The second condition we need to satisfy relates to the timescale factor in the kernel of the Fourier transform. When we apply the imaging condition (28) to this factor we get

$$\frac{-\frac{1}{b}}{2\left(\beta - \frac{1}{2b}\right)} = -\frac{\alpha}{\beta} \equiv m, \tag{30}$$

where m is obviously the magnification factor of the temporal imaging process which is given by the ratio of the input dispersion to the output dispersion. In order to achieve time reversal we must set

$$m = -\frac{\alpha}{\beta} = -1, \tag{31}$$

which is the second condition for time reversal.

With the two conditions for time reversal, Eq. (29) can now be written as

$$\begin{aligned} A_2(z_1 + z_2 + z_{NL}, \tau) &= \frac{r(z_1 + z_{NL})}{(2\pi)^{2.5}} e^{-i\beta a^2} \\ &\times e^{i(2\omega_0 - a)(\tau_a - 2\beta a)} \sqrt{-i2\pi b} e^{i\tau_a^2 (b/2)} \\ &\times \int_{\omega'=-\infty}^{\infty} \tilde{A}_1(0, \omega') e^{i\omega'(-\tau_a)} d\omega' \\ &\times \int_{\omega''=-\infty}^{\infty} \tilde{A}_1(0, \omega'') e^{i\omega''(-\tau_a)} (e^{i\omega'\omega''(2/b)}) d\omega''. \end{aligned} \tag{32}$$

If we now use the bandwidth condition (19) we can neglect the expression $(e^{i\omega'\omega''(2/b)})$ [this is justified by noting that under the bandwidth condition the Fourier coefficients $\tilde{A}_1(0, \omega')$ and $\tilde{A}_1(0, \omega'')$ for ω', ω'' which are larger than $1/\tau_{1,0}$ would be negligible]:

$$\begin{aligned} A_2(z_1 + z_2 + z_{NL}, \tau) &= r(z_1 + z_{NL}) e^{-i\beta a^2} \sqrt{-ib} \\ &\times e^{i(2\omega_0 - a)(\tau_a - 2\beta a)} e^{i\tau_a^2 (b/2)} A_1^2(0, -\tau_a). \end{aligned} \tag{33}$$

With the two time-reversal conditions and with $a = -bt_0$ [see the discussion after Eq. (4)] we get $\tau_a = \tau - 2t_0$ and Eq. (33) becomes

$$\begin{aligned} A_2(z_1 + z_2 + z_{NL}, \tau) &= r(z_1 + z_{NL}) e^{-i\beta a^2} \\ &\times e^{i(2\omega_0 - a)\tau} \sqrt{-ib} e^{i(\tau - 2t_0)^2 (b/2)} A_1^2(0, -\tau + 2t_0). \end{aligned} \tag{34}$$

The final equation constitutes the major result of this work showing that, with the suggested scheme, the SH envelope is proportional to the time-inverted square of the FH envelope.

We recall that this relation still relies on the temporal near-field condition of the temporal Fresnel number $F_t \gg 1$ defined in Eq. (19). This condition can also be treated as a requirement for the SH bandwidth $\Delta\omega_2 = b\tau_{1,0}$ to be much wider than the bandwidth of the FH ($1/\tau_{1,0}$) in order to support a temporal resolution on the order of $\tau_{1,0}$ [44].

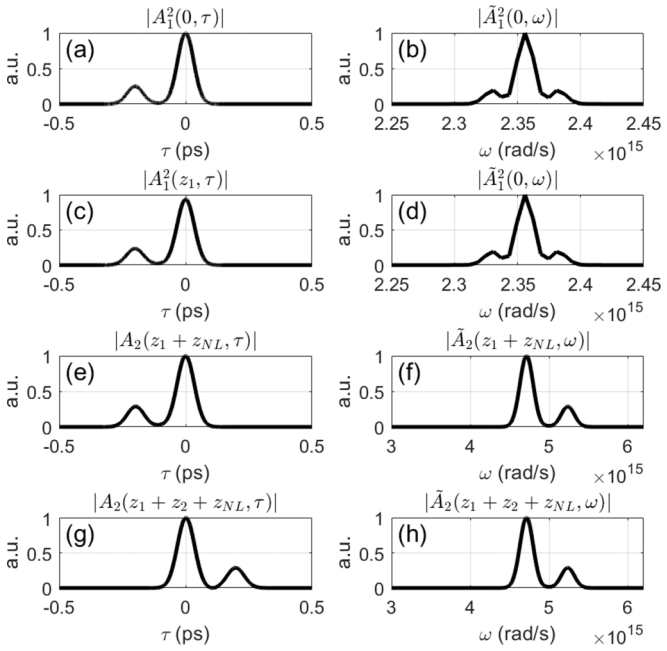

FIG. 2. Demonstration of nonlinear time reversal: (a) temporal and (b) spectral dependence of the FH field at the input to the system, (c) envelope squared of the FH pulse and (d) the FH spectrum at the end of the input dispersion, (e) the SH envelope and (f) the SH spectrum at the end of the nonlinear region, and (g) the SH envelope and (h) the SH spectrum at the end of the output dispersion, showing that the SH envelope is the time-reversed replica of the squared FH envelope. In this simulation $F_t = 30$ and $z_{NL}/l_d = 0.001$.

III. NUMERICAL RESULTS

To demonstrate envelope time-reversal utilizing the format we proposed, we have performed direct numerical integration of the full wave equation (1), implementing the procedure outlined in Ref. [44], to calculate the evolution of the SH in the region of nonlinear interaction. The dispersive regions before and after the nonlinear region were trivially carried analytically.

We simulate propagation of a FH pulse with center wavelength at 800 nm in β barium borate crystal [47] where the ratio between the dispersion length for the SH and coherence length ($l_c = \frac{\pi}{|\Delta k_0|}$) is $\frac{l_d}{l_c} \sim 34$. The FH is a pulse of

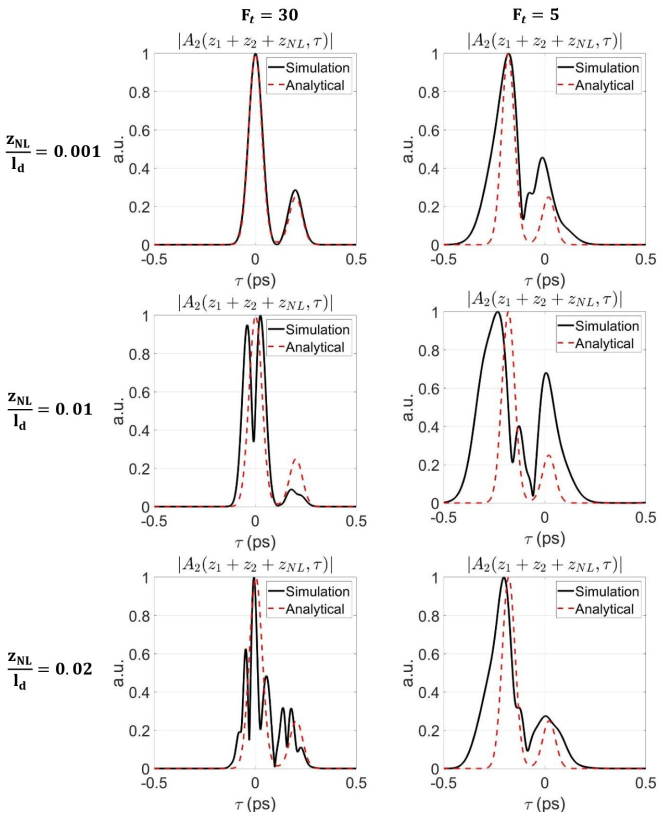

FIG. 3. Effect of the temporal Fresnel number F_t and the nonlinear interaction length to the dispersion length ratio on the nonlinear time-reversal accuracy. All panels show the SH envelope as a function of time, with the FH the same as in Fig. 2, for $F_t = 30$ (left column) and $F_t = 5$ (right column) and $z_{NL}/l_d = 0.001, 0.01, 0.02$ (top, middle, and bottom rows, respectively). The numerical solution is shown with a black solid line while the analytical approximation is shown with a red dashed line.

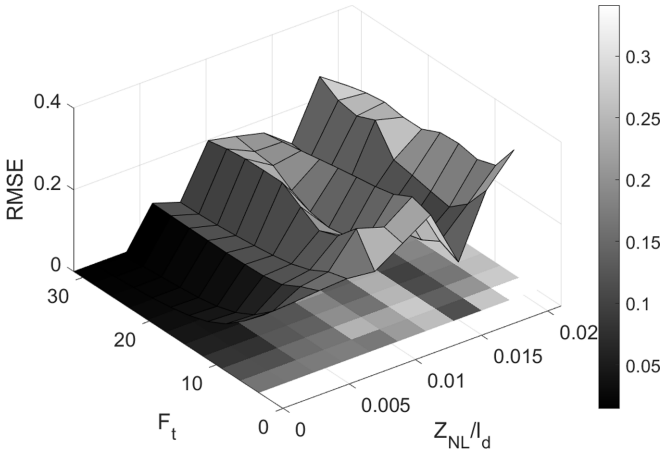

FIG. 4. Accuracy of the nonlinear time reversal. The RMSE calculation between the numerical solution and the analytical approximation of the SH envelope is plotted as a function of the temporal Fresnel number F_t and the ratio of the nonlinear interaction length to the dispersion length. In this simulation we keep $\tau_{1,0} = 0.11$ ps.

approximately 0.5 ps duration with an asymmetric envelope containing two peaks, distanced 0.2 ps apart, taking the middle of the highest FH pulse at $\tau = 0$ and $t_0 = 0$. We choose for the simulation an asymmetric pulse with Gaussian lobes for the FH, although any other waveform can be used in principle.

The envelope squared of the FH pulse is shown in Fig. 2(a) and the FH spectrum is shown in Fig. 2(b). By enforcing the time-reversal conditions given by Eqs. (28) and (31) and applying the dispersive regions with the accelerating QPM modulation realizing the nonlinear time lens described with Eq. (4), a time reversal of the squared envelope is created at the end of the interaction. In order to obtain accurate results without distortions, the chirp rate of the QPM pattern fulfills the requirement of $F_t = \tau_{1,0}^2 b \gg 1$ while the interaction length with the nonlinear crystal obeys $z_{NL} \ll l_d$. Specifically, we choose $F_t = 30$ and $z_{NL}/l_d = 0.001$. At the end of the input dispersion, the field envelope is given by Eq. (9), where the total group-delay dispersion (GDD) is provided by $\alpha = \frac{z_1}{2}\beta_2^{(1)}$. The envelope squared of the FH pulse at the end of the input dispersion is shown in Fig. 2(c) and the FH spectrum is illustrated in Fig. 2(d). In the nonlinear interaction region the SHG process is phase matched and so the amplitude of the SH grows as the interaction length increases. The SH envelope at the end of the nonlinear process is given in Fig. 2(e) and the SH spectrum is given in Fig. 2(f). As $F_t \gg 1$, the squared FH temporal envelope at the end of the input dispersion is mapped to the SH spectrum, with the higher-frequency pulse arriving faster than the lower-frequency pulse. Finally, at the end of the output dispersion, the field envelope is provided by Eq. (26), where the total GDD is given by $\beta = \frac{z_2}{2}\beta_2^{(2)} > 0$. The pulse acquires a positive-frequency sweep and the low-frequency Fourier components travel faster than the high frequencies. The result is that the SH envelope is the time-reversed replica of the squared FH envelope at the end of the output dispersion as shown in Fig. 2(g). The SH spectrum in this case is illustrated in Fig. 2(h).

We further simulated our system for six configurations with two different values of the chirp rate b (included in F_t) and three values for the interaction length in the nonlinear region z_{NL}, keeping $\tau_{1,0} = 0.11$ ps. The SH envelopes formed by the interaction in these cases are shown in Fig. 3. The result of the numerical integration of the SH envelope is shown by a black solid line and that of the analytical approximation (33) by a red dashed line. It is clear that for an accurate nonlinear time reversal the temporal Fresnel number needs to be large and the length of the nonlinear interaction region must be much smaller than the dispersion length within the nonlinear time lens. A more complete representation of these dependences on the quality of the time reversal is given in Fig. 4, which shows the root-mean-square error (RMSE) between the numerical solution and the analytical approximation of the SH envelope.

IV. CONCLUSION

We have shown that under the nondepletion approximation and when higher-order dispersion is negligible, a nonlinear interaction region in which an accelerating spatiotemporal QPM modulation acts as a time lens, accompanied by dispersive elements, can be employed to up-convert a FH field to an envelope time-reversed and squared replica. As opposed to the

work reported in [43], we allow both the SH and FH to propagate along the same world line (same slope in space-time). Thus there is no need at all for group-velocity mismatch. Instead, appropriate dispersive elements are added before and after the accelerating QPM modulation, realizing a nonlinear analog to the well-known temporal imaging scheme with a time lens. The world lines having the same slope for both pump and signal allows better efficiency for the frequency conversion process (when the world lines are of different slopes there is a walkoff in space-time). Furthermore, the selection of the proper input and output dispersion, as well as the chirp rate of the QPM pattern, is dependent on conditions analogous to those of a space imaging system, which takes advantage of the space-time duality between diffraction and dispersion. Such a duality exists also in our nonlinear scheme, which involves signals at different carrier frequencies. The same scheme can also be used to realize temporal magnification between the FH and the SH.

ACKNOWLEDGMENT

The authors acknowledge support from ISF Grant No. 537/19.

APPENDIX: DEVELOPMENT OF THE SECOND HARMONIC FIELD ENVELOPE IN THE TIME DOMAIN

Here we develop the derivation leading from Eq. (26) to Eq. (27). First, apply the inverse Fourier transform on Eq. (26) while substituting Eqs. (25) and (8):

$$A_2(z_1+z_2+z_{NL},\tau)=\frac{r(z_1+z_{NL})}{(2\pi)^{2.5}}\int_{\nu=-\infty}^{\infty}e^{i(\nu+2\omega_0-a)\tau}e^{-i\beta(\nu-a)^2}e^{i\nu^2/2b}d\nu \times\int_{\omega'=-\infty}^{\infty}\int_{\omega''=-\infty}^{\infty}\tilde{A}_1(z_1,\omega')\tilde{A}_1(z_1,\omega'')e^{-i(\omega/b)(\omega'+\omega'')}e^{i(\omega'+\omega'')^2/2b}d\omega' d\omega''. \tag{A1}$$

Switching the order of integration and setting $\tau_a=\tau+2\beta a$, we obtain

$$A_2(z_1+z_2+z_{NL},\tau)=\frac{r(z_1+z_{NL})}{(2\pi)^{2.5}}e^{-i\beta a^2}e^{i(2\omega_0-a)(\tau_a-2\beta a)} \times\int_{\omega'=-\infty}^{\infty}\int_{\omega''=-\infty}^{\infty}\tilde{A}_1(z_1,\omega')\tilde{A}_1(z_1,\omega'')e^{i(\omega'+\omega'')^2/2b}d\omega' d\omega''\int_{\nu=-\infty}^{\infty}e^{i\nu\tau_a}e^{-i\beta\nu^2}e^{i\nu^2/2b}e^{-i(\nu/b)(\omega'+\omega'')}d\nu. \tag{A2}$$

The last integral in Eq. (A2) can be readily evaluated:

$$\begin{aligned}\int_{\nu=-\infty}^{\infty}\exp\left[i\nu\left(\tau_a-\frac{\omega'+\omega''}{b}\right)\right]\exp^{-i\nu^2(\beta-1/2b)}d\nu&=\sqrt{\frac{\pi}{i\left(\beta-\frac{1}{2b}\right)}}\exp\left(i\frac{(\tau_a-\frac{\omega'+\omega''}{b})^2}{4\left(\beta-\frac{1}{2b}\right)}\right)\\&=\sqrt{\frac{\pi}{i\left(\beta-\frac{1}{2b}\right)}}\exp\left(i\frac{\tau_a^2}{4\left(\beta-\frac{1}{2b}\right)}\right)\exp\left(i\frac{\omega'^2\frac{1}{b^2}}{4\left(\beta-\frac{1}{2b}\right)}\right)\exp\left(i\frac{\omega''^2\frac{1}{b^2}}{4\left(\beta-\frac{1}{2b}\right)}\right)\exp\left(i\frac{\omega'\omega''\frac{1}{b^2}}{2\left(\beta-\frac{1}{2b}\right)}\right)\\&\times\exp\left(i\frac{-\tau_a\omega'\frac{1}{b}}{2\left(\beta-\frac{1}{2b}\right)}\right)\exp\left(i\frac{-\tau_a\omega''\frac{1}{b}}{2\left(\beta-\frac{1}{2b}\right)}\right).\end{aligned} \tag{A3}$$

Using this result in Eq. (A2) gives

$$\begin{aligned}A_2(z_1+z_2+z_{NL},\tau)=\frac{r(z_1+z_{NL})}{(2\pi)^{2.5}}e^{-i\beta a^2}e^{i(2\omega_0-a)(\tau_a-2\beta a)}&\sqrt{\frac{\pi}{i\left(\beta-\frac{1}{2b}\right)}}\exp\left(i\frac{\tau_a^2}{4\left(\beta-\frac{1}{2b}\right)}\right)\\&\times\int_{\omega'=-\infty}^{\infty}\tilde{A}_1(z_1,\omega')e^{i\omega'^2/2b}\exp\left(i\frac{\omega'^2\frac{1}{b^2}}{4\left(\beta-\frac{1}{2b}\right)}\right)\exp\left(i\frac{-\tau_a\omega'\frac{1}{b}}{2\left(\beta-\frac{1}{2b}\right)}\right)d\omega'\\&\times\int_{\omega''=-\infty}^{\infty}\tilde{A}_1(z_1,\omega'')e^{i\omega''^2/2b}\exp\left(i\frac{\omega''^2\frac{1}{b^2}}{4\left(\beta-\frac{1}{2b}\right)}\right)\exp^{i\frac{-\tau_a\omega''\frac{1}{b}}{2\left(\beta-\frac{1}{2b}\right)}}\\&\times\left[\exp\left(i\frac{\omega'\omega''\frac{1}{b^2}}{2\left(\beta-\frac{1}{2b}\right)}\right)\exp\left(i\frac{\omega'\omega''}{b}\right)\right]d\omega''.\end{aligned} \tag{A4}$$

Finally, by using Eqs. (5) and (6) we get

$$
\begin{aligned}
A_2(z_1+z_2+z_{NL},\tau) = {} & \frac{r(z_1+z_{NL})}{(2\pi)^{2.5}} e^{-i\beta a^2} e^{i(2\omega_0-a)(\tau_a-2\beta a)} \sqrt{\frac{\pi}{i\left(\beta-\frac{1}{2b}\right)}} \exp\left(i\frac{\tau_a^2}{4\left(\beta-\frac{1}{2b}\right)}\right) \\
& \times \int_{\omega'=-\infty}^{\infty} \tilde{A}_1(0,\omega') \exp\left[i\omega'^2\left(-\alpha+\frac{1}{2b}+\frac{\frac{1}{b^2}}{4\left(\beta-\frac{1}{2b}\right)}\right)\right] \exp\left[i\omega'\left(\frac{-\frac{1}{b}}{2\left(\beta-\frac{1}{2b}\right)}\right)\tau_a\right] d\omega' \\
& \times \int_{\omega''=-\infty}^{\infty} \tilde{A}_1(0,\omega'') \exp\left[i\omega''^2\left(-\alpha+\frac{1}{2b}+\frac{\frac{1}{b^2}}{4\left(\beta-\frac{1}{2b}\right)}\right)\right] \\
& \times \exp\left[i\omega''\left(\frac{-\frac{1}{b}}{2\left(\beta-\frac{1}{2b}\right)}\right)\tau_a\right]\left\{\exp\left[i\omega'\omega''\left(\frac{\frac{1}{b^2}}{2\left(\beta-\frac{1}{2b}\right)}+\frac{1}{b}\right)\right]\right\} d\omega''. \qquad \text{(A5)}
\end{aligned}
$$

[1] G. S. Agarwal, A. T. Friberg, and E. Wolf, J. Opt. Soc. Am. **73**, 529 (1983).
[2] M. Fink, Sci. Am. **281**, 91 (1999).
[3] *Imaging of Complex Media with Acoustic and Seismic Waves*, edited by M. Fink, W. A. Kuperman, J.-P. Montagner, and A. Tourin, Topics in Applied Physics Vol. 84 (Springer, Berlin, 2002).
[4] O. Katz, E. Small, Y. Bromberg, and Y. Silberberg, Nat. Photon. **5**, 372 (2011).
[5] J. Aulbach, B. Gjonaj, P. M. Johnson, A. P. Mosk, and A. Lagendijk, Phys. Rev. Lett. **106**, 103901 (2011).
[6] M. I. Stockman and X. Li, *Frontiers in Optics 2008/Laser Science XXIV/Plasmonics and Metamaterials/Optical Fabrication and Testing* (Optical Society of America, Washington, DC, 2008), p. MTuB4.
[7] M. Fink, J. Phys. D **26**, 1333 (1993).
[8] J. Pendry, Science **322**, 71 (2008).
[9] G. Lerosey, J. Rosny, A. Tourin, and M. Fink, Science **315**, 1120 (2007).
[10] X. Li and M. I. Stockman, Phys. Rev. B **77**, 195109 (2008).
[11] Z. Yaqoob, D. Psaltis, M. Feld, and C. Yang, Nat. Photon. **2**, 110 (2008).
[12] Y. Kajiwara, K. Harii, S. Takahashi, J. Ohe, K. Uchida, M. Mizuguchi, H. Umezawa, H. Kawai, K. Ando, K. Takanashi, S. Maekawa, and E. Saitoh, Nature (London) **464**, 262 (2010).
[13] F. Cucchietti, J. Opt. Soc. Am. B **27**, A30 (2010).
[14] A. Yariv, D. Fekete, and D. M. Pepper, Opt. Lett. **4**, 52 (1979).
[15] D. A. B. Miller, Opt. Lett. **5**, 300 (1980).
[16] O. Kuzucu, Y. Okawachi, R. Salem, M. A. Foster, A. C. Turner-Foster, M. Lipson, and A. L. Gaeta, Opt. Express **17**, 20605 (2009).
[17] D. Marom, D. Panasenko, R. Rokitski, P.-C. Sun, and Y. Fainman, Opt. Lett. **25**, 132 (2000).
[18] C. Joubert, M. L. Roblin, and R. Grousson, Appl. Opt. **28**, 4604 (1989).
[19] A. Weiner, D. Leaird, D. Reitze, and E. Paek, IEEE J. Quantum Electron. **28**, 2251 (1992).
[20] M. F. Yanik and S. Fan, Phys. Rev. Lett. **93**, 173903 (2004).
[21] S. Longhi, Phys. Rev. E **75**, 026606 (2007).
[22] Y. Sivan and J. B. Pendry, Phys. Rev. Lett. **106**, 193902 (2011).
[23] S. Chin, N. Primerov, K. Y. Song, L. Thévenaz, M. Santagiustina, and L. Ursini, *Advanced Photonics and Renewable Energy* (Optical Society of America, Washington, DC, 2010), p. NThA6.
[24] Y. Zheng, H. Ren, W. Wan, and X. Chen, Sci. Rep. **3**, 3245 (2013).
[25] A. V. Chumak, V. S. Tiberkevich, A. D. Karenowska, A. A. Serga, J. F. Gregg, A. N. Slavin, and B. Hillebrands, Nat. Commun. **1**, 141 (2010).
[26] S. Fan and M. F. Yanik, *Proceedings of the 31st European Conference on Optical Communication, Glasgow, 2005* (Institution of Electrical Engineers, London, 2005), Vol. 5, p. 3.
[27] B. Kolner, IEEE J. Quantum Electron. **30**, 1951 (1994).
[28] C. V. Bennett and B. H. Kolner, Opt. Lett. **24**, 783 (1999).
[29] T. Jannson, Opt. Lett. **8**, 232 (1983).
[30] M. T. Kauffman, W. C. Banyai, A. A. Godil, and D. M. Bloom, Appl. Phys. Lett. **64**, 270 (1994).
[31] L. Mouradian, F. Louradour, V. Messager, A. Barthelemy, and C. Froehly, IEEE J. Quantum Electron. **36**, 795 (2000).
[32] C. Bennett and B. Kolner, IEEE J. Quantum Electron. **36**, 430 (2000).
[33] R. W. Boyd, in *Nonlinear Optics*, 3rd ed., edited by R. W. Boyd (Academic, Burlington, 2008), pp. 69–133.
[34] J. A. Armstrong, N. Bloembergen, J. Ducuing, and P. S. Pershan, Phys. Rev. **127**, 1918 (1962).
[35] M. A. Foster, R. Salem, D. F. Geraghty, A. Turner-Foster, M. Lipson, and A. L. Gaeta, Nature (London) **456**, 81 (2008).
[36] R. Lifshitz, A. Arie, and A. Bahabad, Phys. Rev. Lett. **95**, 133901 (2005).
[37] A. Bahabad, M. M. Murnane, and H. C. Kapteyn, Nat. Photon. **4**, 570 (2010).
[38] X. Zhang, A. Lytle, T. Popmintchev, X. Zhou, H. Kapteyn, M. Murnane, and O. Cohen, Nat. Phys. **3**, 270 (2007).
[39] S. Akturk, X. Gu, P. Bowlan, and R. Trebino, J. Opt. **12**, 9 (2010).
[40] A. Bahabad, M. M. Murnane, and H. C. Kapteyn, Phys. Rev. A **84**, 033819 (2011).
[41] J. Peatross, S. Voronov, and I. Prokopovich, Opt. Express **1**, 114 (1997).

[42] A. Bahabad, O. Cohen, M. M. Murnane, and H. C. Kapteyn, Opt. Express **16**, 15923 (2008).
[43] M. Yachini, B. Malomed, and A. Bahabad, ACS Photon. **3**, 2017 (2016).
[44] M. Konsens and A. Bahabad, Phys. Rev. A **93**, 023823 (2016).
[45] J. Azana, N. Berger, B. Levit, and B. Fischer, IEEE Photon. Technol. Lett. **16**, 882 (2004).
[46] L. Ménager, I. Lorgeré, J.-L. L. Gouët, R. K. Mohan, and S. Kröll, Opt. Lett. **24**, 927 (1999).
[47] D. Eimerl, L. Davis, S. Velsko, E. K. Graham, and A. Zalkin, J. Appl. Phys. **62**, 1968 (1987).